Hindawi
Advances in Civil Engineering
Volume 2022, Article ID 5361199, 11 pages
https://doi.org/10.1155/2022/5361199

Research Article

Research on Natural Foundation Bearing Capacity and Foundation Pit Settlement of Prefabricated Utility Tunnel

Zengshan Wang,[1] Yanying Wang,[1] Weike Huang,[2] Hongwei Shan,[2] and Li Zhu[3]

[1]*CCCC Xiong'an Investment Co., Ltd., Baoding, Hebei 071700, China*
[2]*CCCC-SHEC Sixth Engineering Co., Ltd., Xi'an, Shaanxi 710075, China*
[3]*CCCC-SHEC Engineering Design and Research Institute, Xi'an 710199, China*

Correspondence should be addressed to Li Zhu; zhuli10@ccccltd.cn

Received 23 February 2022; Accepted 23 March 2022; Published 4 April 2022

Academic Editor: Gaofeng Song

Prefabricated assembled integrated pipe corridor has the significant advantages of fast assembly, controlled quality of factory prefabricated forming, short construction period, energy saving and environmental protection compared with on-site casting. In this paper, a shallow plate load field test was carried out to test the bearing capacity of the natural foundation of the assembled pipe corridor and a numerical simulation analysis of the settlement of the substrate was carried out in combination with the typical local soft soil geological conditions, using the JXSG-6 beam making site in Gu'an South of the Beijing-Xiong Intercity Railway in Xiong'an New Area as the test site. The results of the study show that: during the vertical loading to 320 kPa, the overall displacement settlement of the foundation soil of each experimental group is small, mainly elastic deformation, and the final settlement of each test group is 6.68 mm, 10.89 mm and 5.38 mm respectively, with no cracks and no damage to the foundation soil. According to the calculation of the straight line section of the load settlement data, the average value of the foundation soil bearing capacity deformation modulus is 43.1 MPa, and the average value of the foundation stiffness of the 0.8 m diameter circular bearing plate is 78.2 MPa/m, which can provide a parameter basis for the structural design of the pipe corridor and the subsequent superstructure test calculation. However, due to the large stiffness difference between the structure of the pipe gallery and the soil, the soil settlement deformation process and the pipe gallery relative displacement, the shear effect on both sides of the pipe gallery; differential settlement under the influence of the local surface of the pipe gallery may occur tensile damage, the maximum displacement concentrated on both sides of the pit reached 0.6 mm, in the acceptable range. Therefore, the lower base of the pipe corridor has good bearing capacity and can meet the construction requirements of the installation stage of the integrated pipe corridor sections.

1. Introduction

The Xiongan New Area is another new area of national significance, following the Shenzhen Special Economic Zone and Shanghai Pudong New Area. As an important part of the urban infrastructure construction in the Xiongan New Area, the construction of an underground integrated pipe corridor is of great significance in ensuring the safety of municipal pipelines, improving the utilisation of underground space, beautifying the urban environment and avoiding repeated excavations on the road surface [1–3]. The typical assembled pipe corridor structure designed by China Communications Construction Group is 15.9 m in width, 4.9 m in height and 6 m in length for a single longitudinal section, which is the largest cross-section and the largest lifting tonnage in China [4, 5]. At present, the research on the support structure deformation, pit bottom uplift and surface settlement in the process of foundation excavation is more mature, but for the integrated pipe corridor project not only needs to focus on the safety of foundation excavation, but also needs to study in depth the settlement of the integrated pipe corridor in the foundation pit itself [6–10].

With the construction of integrated pipe corridors in full swing in recent years, especially prefabricated pipe corridors

after installation, settlement at the joints due to differences in foundation bearing capacity, resulting in incidents such as leakage of integrated pipe corridors are common [11, 12]. Huang and Fan [13] studied the influence of the depth of foundation reinforcement on the force performance of the integrated pipe corridor structure on soft ground, and the vertical displacement of the integrated pipe corridor structure and the vertical displacement of the surface soil within the width were influenced by the depth of foundation reinforcement; Hu et al. [14] studied the influence of the elastic modulus of the weak soil layer on the force performance of the prefabricated assembled integrated pipe corridor, and the results showed that the reduction of the elastic modulus of the weak soil layer would The results show that the reduction of the elastic modulus of the weak soil layer will aggravate the uneven settlement of the corridor, and the weak soil layer has a greater influence on the longitudinal and transverse internal forces of the corridor structure; Wang studied the load deformation law of the prefabricated integrated corridor structure under uneven settlement conditions with the [15] help of Midas Gen finite element simulation software.

In this paper, a shallow plate load field test was carried out on the bedding layer in the construction area of the pipe corridor, using the JXSG-6 beam making site in Gu'an South of the Xiongan New Area Beijing-Xiongan Intercity Railway as the test site, and the test results were obtained. The COMSOL software was used to establish a numerical model to monitor the stress and displacement of the foundation pit to obtain the overall map and slice map of the stress and displacement distribution characteristics respectively, which were analysed to obtain the settlement characteristics of the foundation pit. This study can effectively guarantee the safe and rapid construction of the integrated pipe corridor section installation stage and provide practical guidance for the integrated pipe corridor project.

2. Project Overview

The project site is located in NA8 Road, the start-up area of Xiongan New Area, Hebei Province. This test is mainly in the NA8 line NA8K1 + 564 to NA8K2 + 380 section of the pipe corridor section installation of the whole process of key technology test research. The excavation base of the assembled integrated pipe corridor pit is in-situ soil with bedding treatment on it. Therefore, the bearing performance of the original soil of the pit is directly related to the treatment measures of the upper bedding layer, and whether the assembled integrated pipe corridor meets the settlement control standard [16, 17]. According to the preliminary survey site, the base elevation -2.085 m, the original ground elevation 7.911 m (as shown in Figure 1), three groups of test site are to powder clay, powder soil for the bearing layer, according to the survey design specification, powder clay, powder ground foundation bearing capacity characteristic value for 130 kPa, the test choose the bearing capacity characteristic value of 2.5 times, that is, 320 kPa as the loading limit value.

3. Shallow Plate Load Test

The shallow plate load test is an in-situ test method [18] to measure the pressure and deformation characteristics of the foundation soil by applying a load to the foundation soil step by step on a certain area of bearing plate, which can reflect the comprehensive characteristics of the strength and deformation of the foundation soil in the range of 1.5 to 2.0 times the diameter or width of the bearing plate under the bearing plate. The test was carried [19] out on the site of the integrated corridor. The test was carried out on the in-situ soil of the excavated pit in the construction area of the integrated pipe corridor, and the shallow plate load test was carried out.

3.1. Basic Principle of Test. The pressure-settlement curve (P-S curve) obtained from the typical plate load test can be divided into three stages:

(1) Linear deformation stage: when the pressure is less than the proportional limit pressure p0, P–S shows a linear relationship. At this time, the shear stress generated at any point in the loaded soil is less than the shear strength of the soil. The deformation of the soil is mainly caused by the decrease of the void in the soil, and the deformation of the soil is mainly vertical compression.

(2) Shear deformation stage: when the pressure is greater than $p0$ and less than the limit pressure pu, the P-S relationship changes from a straight line to a curve relationship. The slope of the P-S relationship curve increases with the increase of pressure p, and the soil is in addition to vertical compression. In the edge of the plate has a small range of soil shear stress reached or exceeded the shear strength of soil, and began to develop to the surrounding soil. The deformation is caused by both vertical compression and shear deformation of soil particles.

(3) Failure stage: when the pressure is greater than the ultimate pressure pu, the settlement increases sharply. Even if the pressure is no longer increased, the bearing plate is still sinking. The continuous sliding surface is formed inside the soil, and the uplift and annular or radial cracks occur around the bearing plate. The shear stress at each point in the sliding soil reaches or exceeds the shear strength of the soil.

3.2. Test Technical Requirements

(1) Load test should adopt circular rigid bearing plate, according to the soft and hard soil or rock fracture density to choose the appropriate size; the area of bearing plate in shallow plate loading test of soil should be greater than 0.25 m^2.

(2) The test pit can be square and circular, and its width is greater than three times the width of the bearing plate, so is its diameter. The measured object should

Figure 1: Site survey map.

avoid disturbance and keep the original state as far as possible. The sand cushion with thickness less than 20 mm should be laid at the bottom of the test pit to leveling and quickly install the equipment. The settlement measuring instrument is uniformly installed.

(3) The maximum loading should not be less than twice of the design requirements, and the loading classification should be greater than 7. Generally, the equal incremental load applied is about 1/10 of the predicted ultimate load, and the measurement accuracy of the load should be at the maximum load of ±1%.

(4) The loading methods include conventional slow method, fast method and equal settlement rate method. This paper only introduces the slow method. When the test object is soil, the settlement is measured at intervals of 10, 10, 10, 15 and 15 after each load is applied, and then the settlement is measured at intervals of 30 min. When the settlement is less than or equal to 0.1 mm per hour after continuous reading for two hours, it can be considered that the settlement has reached the relatively stable standard and the next load is applied. When the test object is rock mass, the settlement is measured once at intervals of 1, 2, 5 min, and then every 30 min. When the reading difference of three consecutive times is less than or equal to 0.01 mm, it can be considered that the settlement has reached the relatively stable standard and the next load is applied.

(5) When one of the following cases occurs, the test can be terminated, and the load at the termination is the pilot limit load. When the soil around the bearing plate is obviously lateral extrusion, the surrounding rock and soil appear obvious uplift or radial cracks continue to develop; the settlement of the load at this level increases sharply, which is five times larger than that of the load at the upper level, that is, there is a sharp drop in the P-S curve; when a certain load does not meet the stability standard for 24 hours; when the ratio of the total settlement to the diameter of the bearing plate $s/b > 0.06$.

3.3. Test Scheme and Equipment. The rock and soil at the bottom of the test pit or test well should be avoided from disturbance and kept in its original structure and natural moisture, and a medium or coarse sand bedding layer of not more than 20 mm should be laid under the pressure plate to level it and make uniform contact with the soil, and test equipment should be installed as soon as possible, as shown in Figure 2.

The equipment arrangement mainly includes: loading and pressure stabilisation system, counterforce platform

(a) (b)

Figure 2: Positioning (a) with medium coarse sand leveling (b).

system and observation system. The loading method adopts the slow maintenance load method, using the four vertical bearing plates installed in the bearing plate edge length direction percentage table or displacement meter to observe and record the settlement, to determine the load added at each level by the oil pressure gauge on the jack. The load is applied by means of jack ballast test equipment, through high pressure oil pump, ballast platform as a counterforce device, the pressure is steadily transferred to the bearing plate, the equipment consists of the following three parts: (a) loading and pressure stabilisation system: by the bearing plate, loading jack, column, pressure stabiliser and tripod to support the pressure stabiliser. The loading jack, pressure stabiliser, oil storage tank and high pressure oil pump are connected by high pressure hoses to form an oil circuit system. (b) Counter force platform system: including two parts: truss and ballast test block, the truss consists of central column sleeve, depth adjusting screw, inclined support tube, etc. (c) Observation system: four displacement meters are arranged at each corner of the straight side of the loading plate for settlement observation with an accuracy of not less than ±0.01 mm.

3.4. Loading and Observation Scheme. The test was carried out using the existing assembled pavement concrete piles on-site, with a prepressure load of 5% of the maximum load and a prepressure time of 5 min. After completion of the prepressure, the piles were unloaded to zero and the initial readings of the displacement measuring instruments were readjusted to zero.

According to the Technical Specification for Building Foundation Inspection JGJ 340-2015, the total loading of the load test is generally not less than 2 times the design bearing capacity, and this test is loaded [19] according to 3 times the design bearing capacity. The ultimate load in the test was 400 kPa as the front leg pad of the corridor machine was designed and controlled in accordance with the dimension of the base pressure not exceeding 130 kPa. The load was loaded in 10 equal steps using stacking blocks, each in 40 kPa increments, and the accuracy of the load measurement was not less than ±1% of the maximum load.

After each level of loading is completed, three settlement measurements are taken at 10 min intervals, then two readings are taken at 15 min intervals and thereafter every 30 min until the settlement is less than 0.1 mm per hour continuously, then the settlement is considered to have reached a relatively stable standard and the next level of loading is applied. The conditions for termination of the test include: significant lateral extrusion of the soil around the bearing plate, significant uplift of the surrounding rock and soil or continued development of radial cracks; a sharp increase in settlement, the appearance of landfall sections on the load-settlement curve and settlement at this level of loading greater than five times the settlement at the previous level of loading; the settlement rate does not reach the relative stability standard for 24 hours under a particular level of loading; the ratio of the total settlement to the diameter (or width) of the bearing plate exceeds 0.06. If one of the above conditions is met, the corresponding previous level of load is the ultimate load. After the test has been completed, the unloading is carried out in three equal stages. After each stage of unloading, the rebound value is read at 15 min intervals, and after two readings, the next stage of loading is read at 30 min intervals. After all unloading, the rebound value is read again at 3 h intervals.

3.5. Analysis of Experimental Data. For the determination of the characteristic value of foundation bearing capacity, when there is a proportional limit on the curve, take the load value corresponding to the proportional limit; when the ultimate load is less than twice the load value corresponding to the proportional limit, take half of the ultimate load value; when it cannot be determined according to the requirements of the above two paragraphs, take the load corresponding to $s/b = 0.01$, but its value should not be greater than half of the maximum loading; when the measured values of the three test points When the extreme difference between the measured values of the three test points does not exceed 30% of their average value, the average value is taken as the characteristic value of the foundation bearing capacity of the soil layer. The modulus of deformation E_0 for the shallow

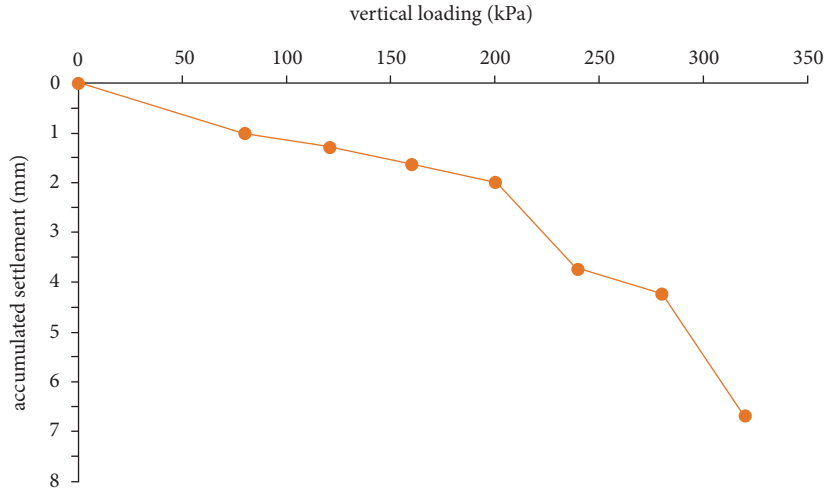

Figure 3: Pictures of test loading process.

Table 1: Load settlement data curve.

Loading (kPa)	0	80	120	160	200	240	280	320
Level settlement (mm)	0.00	1.01	0.27	0.34	0.37	1.75	0.49	2.45
Accumulated settlement (mm)	0.00	1.01	1.28	1.62	1.99	3.74	4.23	6.68

plate load test is calculated according to the following formula [20–22].

$$E_0 = I_0\left(1 - v^2\right)\frac{pd}{s}, \quad (1)$$

where, I_0—shape factor of the rigid bearing plate; v—Poisson's ratio of the soil; d—edge length of the bearing plate, m; p—load for linear section of P-S curve, kPa; s—settlement corresponding to p, mm.

3.6. Main Test Results. The load test of the foundation bearing capacity of the assembled integrated pipe corridor, the cumulative loading time on-site were 35 h, 49 h, 26.5 h. According to the calculation of the difference of the test data, the settlement of the three groups of tests was 1.37, 2.34 mm, 2.34 mm and 2.34 mm respectively for the load value of 130 kPa.1.37 mm, 2.34 mm When loaded to 320 kPa, the cumulative settlement of the foundation was 6.68 mm, 10.89 mm and 5.38 mm respectively, with a small total settlement. The modulus of mat deformation was calculated according to equation (1) above, where $I_0 = 0.785$, $v = 0.35$, $d = 0.8$ m, $p = 120$ kPa, $s = 4.23$ mm, 8.43 mm, 4.32 mm, and the calculated modulus of mat deformation $E_0 = 51.7$ MPa, 33.2 MPa, 44.4 MPa, with the mean value of 43.1 MPa. The foundation stiffness p/s of the 0.8 m diameter circular bearing plate are 94 MPa/m, 60 MPa/m and 81 MPa/m respectively, and the average value is 78.2 MPa/m.

The first set of test data and P-S diagram are shown in Figure 3. According to the test data (As shown in Table 1), it can be seen that when the load reaches 320 kPa, the settlement of this stage is five times that of the upper stage. The termination of loading can be regarded as the occurrence of ultimate failure. The upper stage 280 kPa is taken as the ultimate load, and 1/2 is the eigenvalue of ultimate bearing capacity, namely 140 kPa.

The second group of test data and P-S diagram, as shown in Figure 4, according to the test data (As shown in Table 2), it can be seen that when the loading to 320 kPa, there is no termination of loading conditions, to achieve a relatively stable standard termination of loading, the bearing capacity of the test point reached the survey design value of 160 kPa.

The third group of test data and P-S diagram, as shown in Figure 5, according to the test data(As shown in Table 3), it can be seen that when the loading to320 kPa, there is no termination of loading conditions, to achieve a relatively stable standard termination of loading, the bearing capacity of the test point reached the survey design value of 160 kPa.Take three groups of data average value as foundation bearing capacity characteristic value of 153 kPa.

4. Numerical Simulation Study of Foundation Settlement

4.1. Numerical Model and Boundary Conditions. The integrated pipe corridor stage size single section is 4 compartment pipe corridor, the width of this simulation is selected as 4 m small prefabricated pipe corridor, the section length is 13.0 m, the height is 4.2 m, the dead weight is 201 t. In the field construction, the main structure of the pipe corridor using C45 high performance concrete, the pipe corridor model in this numerical simulation using nonvariable type material for reduction. Also in the modelling process the mattress bedding and

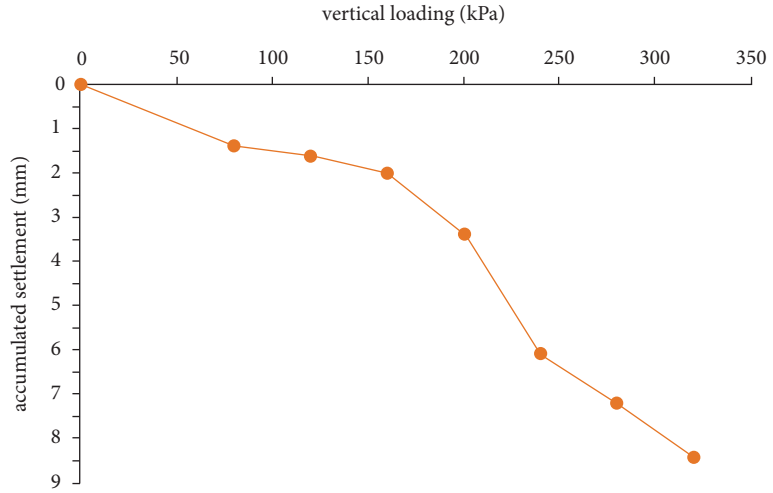

Figure 4: Pictures of test loading process.

Table 2: Load settlement data curve.

Loading (kPa)	0	40	80	120	160	200	240	280	320
Level settlement (mm)	0.00	1.38	0.23	0.38	1.39	2.70	1.12	1.23	2.46
Accumulated settlement (mm)	0.00	1.38	1.61	1.99	3.38	6.08	7.20	8.43	10.89

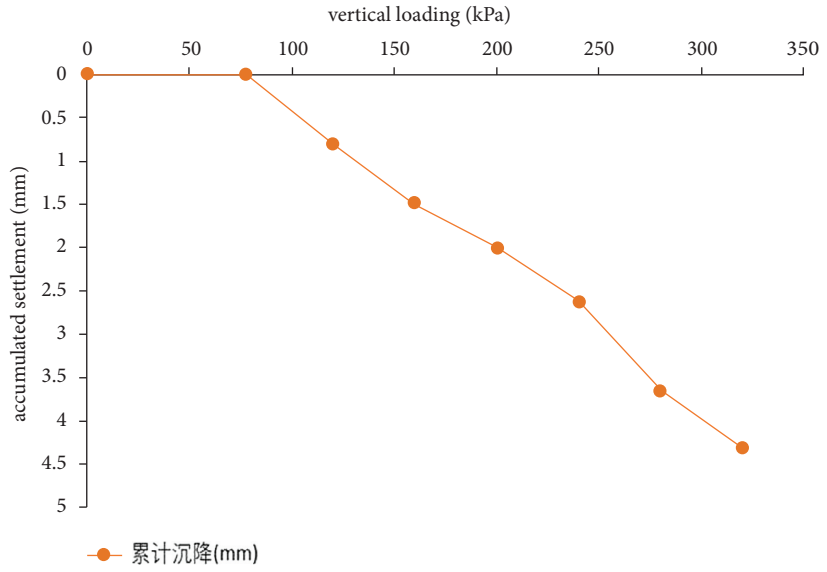

Figure 5: Pictures of test loading process.

subgrade were reasonably simplified due to the small size of only 10 cm–20 cm. According to the analysis of the borehole sampling, the powdered clay and powdered soil are the bearing layer, therefore this simulation will be set up according to the parameters of powdered clay for the stratum underneath the pipe corridor, with the dimensions of length x width x height, $20 \times 6 \times 3$. The numerical model was established using COMSOL software as shown in Figure 6. According to the ground investigation data, test data, combined with the experience of similar projects and reference literature, the material parameters were determined comprehensively.

4.2. Numerical Simulation Results and Analysis

4.2.1. Pit Stress Analysis. By monitoring the stresses, a characteristic map of the stress distribution is obtained, as shown in Figure 7.

It can be seen from Figure 7 that the downward tangential stress is mainly generated at the interface between the two sides of the pipe gallery. The positive and negative signs of the stress are mainly caused by the different local coordinate systems of the interface element. When the direction of the tangential stress is

Table 3: Load settlement data curve.

Loading (kPa)	0	40	80	120	160	200	240	280	320
Level settlement (mm)	0.00	0.00	0.80	0.69	0.51	0.62	1.04	0.66	1.06
Accumulated settlement (mm)	0.00	0.00	0.80	1.49	2.00	2.62	3.66	4.32	5.38

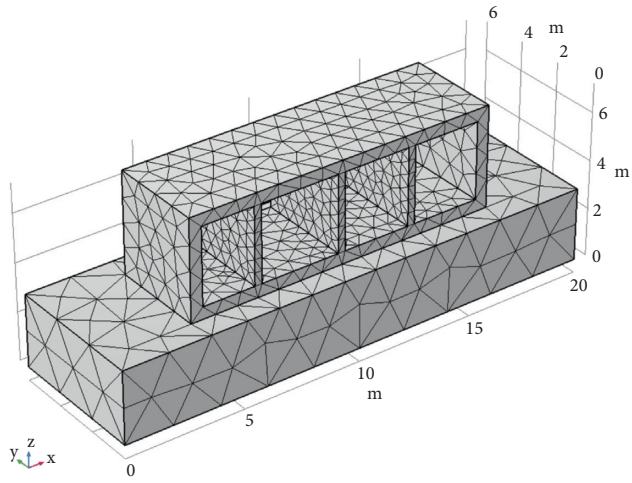

Figure 6: Numerical modelling.

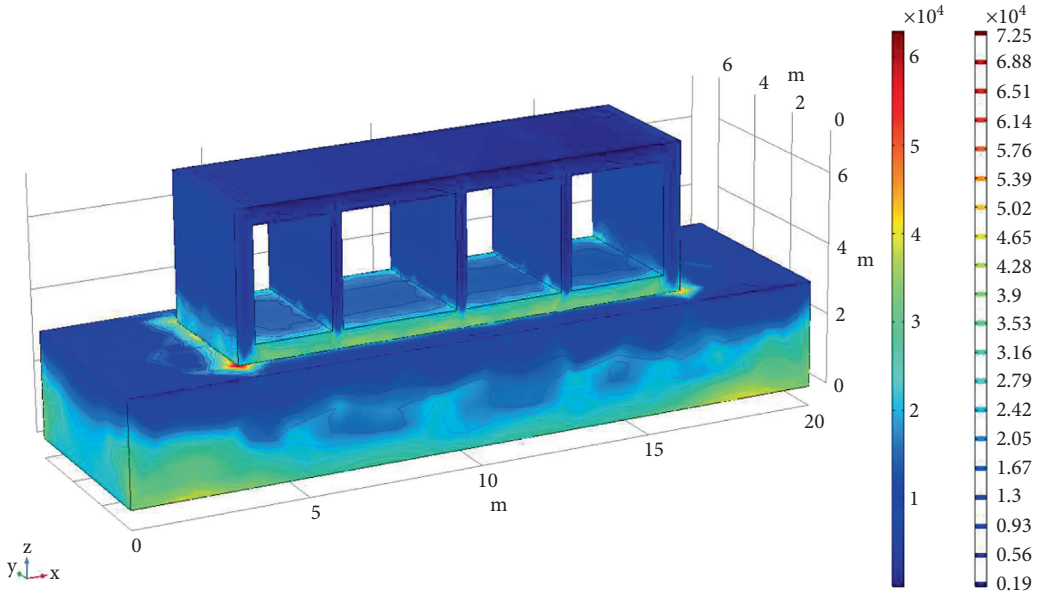

(a)

Figure 7: Continued.

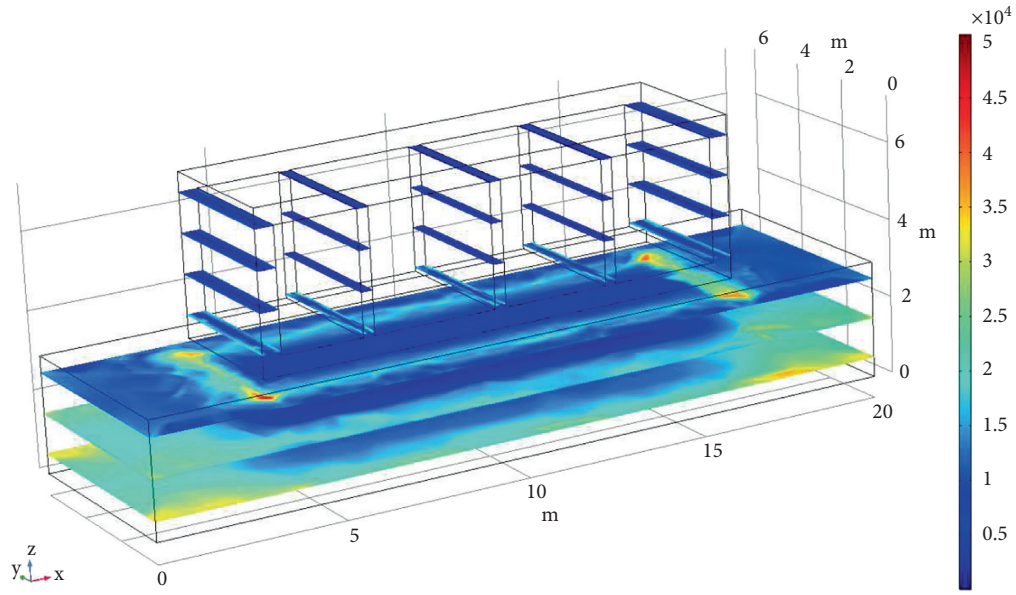

(b)

Figure 7: Stress distribution characteristics. (a) Overall view. (b) Slice map.

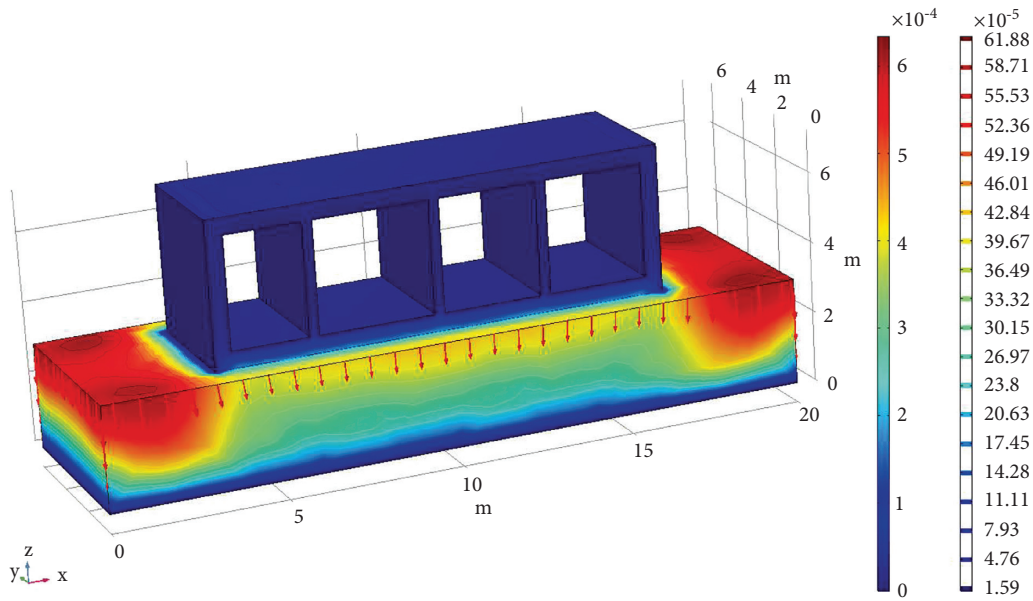

(a)

Figure 8: Continued.

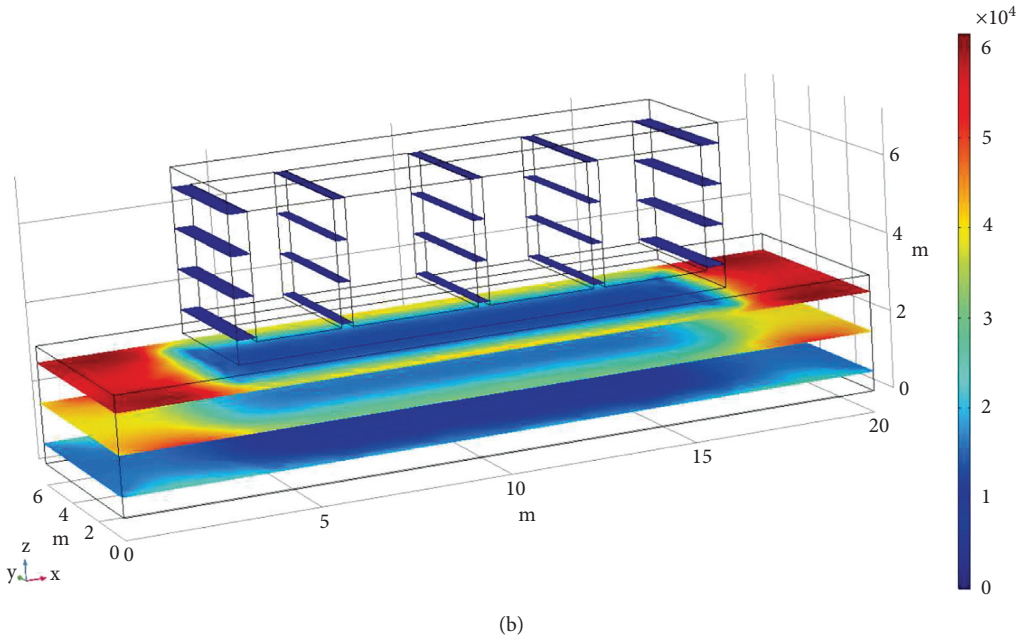

(b)

Figure 8: Map of displacement distribution characteristics. (a) Overall view. (b) Slice map.

consistent with the direction of the local coordinate axis, it is positive, and vice versa. Therefore, although the tangential stress is positive on the left and negative on the right, it is actually downward. The stress of the side wall near the intersection of the two sides of the pipe gallery and the rock layer is large. From the stress slice diagram in Figure 7(b), it can be seen that taking the interface at the right wall of the first section of the pipe gallery as an example, the bottom stress of the side wall is 25 kPa–45 kPa, which is positive and the direction is upward. The tangential stress at the top of the sidewall is −30 kPa~−60 kPa, negative and downward. It can be speculated from the stress diagram that the stress of the two sides and the four corners of the contact between the pipe gallery and the base is relatively concentrated, which may cause large displacement. The bearing capacity of the undisturbed soil of the foundation pit is directly related to the treatment measures of the upper cushion. Therefore, it is necessary to strengthen the cushion treatment of this part.

4.2.2. Foundation Pit Displacement Analysis. By monitoring the displacements, a map of the displacement distribution characteristics was obtained, as shown in Figure 8.

Due to the stiffness difference between the pipe gallery structure and the surrounding soil, the pipe gallery structure also plays a certain role in limiting the settlement of the surrounding soil. The maximum surface settlement below the segmental pipe gallery is about 0.2 mm, which is smaller than that of the surrounding soil. Figure 8(b) Slice diagram shows that the vertical displacement of the soil below the elevation of the pipe gallery bottom plate, from the cross-sectional direction of the pipe gallery (z axis direction), the settlement of the soil on both sides of the bottom plate at the end of the segmental pipe gallery is the largest, up to 0.6 mm, by contrast, the settlement of the soil at the bottom plate of the center of the pipe gallery is smaller, about 0.2 mm; that is, because of the laying of the segmental pipe gallery, the land on both sides of the base has been squeezed, resulting in displacement, and larger than the land under the pipe gallery. In conclusion, the overall displacement is in a stable state, and the main displacement occurs in the corners and on both sides. It is necessary to pay attention to the treatment of the foundation in this part. The settlement of the bottom and foundation of different pipe gallery will directly affect the overall mechanical performance of the pipe gallery. If there is a certain range of cushion separation will lead to uneven stress of the pipe gallery, affecting the performance of the use, serious concrete cracking, affecting the normal use and safety of the structure [23].

5. Conclusion

(1) Combined with the existing ground survey report and on-site observation, the current test pit of CCCC (construction pit of integrated pipe corridor) and CCCC is located in the same area of Rongdong, and the two are close to each other, and the elevation is roughly in the same range (test site elevation −2.085 m; original ground elevation 7.911 m), and most of the soils are powder and powder clay. The results are a guide to the design of the bedding layer for the assembled integrated pipe corridor.

(2) According to the ground survey, it is known that the characteristic value of foundation bearing capacity of

powder soil and powder clay is 130 kPa, according to the specification, the total loading amount is generally not less than 2 times of the design bearing capacity, this test is considered according to 2.5 times of the design bearing capacity, i.e. 320 kPa (diameter of bearing plate 0.8 m). Test results show that the vertical loading to 320 kPa process, each experimental group foundation soil overall displacement settlement is small, mainly for the elastic deformation, foundation soil no cracks, no damage phenomenon, take three groups of data average value as foundation bearing capacity characteristic value of 153 kPa.

(3) According to the calculation of the straight line section of the load settlement data, the foundation soil bearing capacity deformation modulus is $E = 51.7$ MPa, 33.2 MPa, 44.4 MPa, and the average value of deformation modulus is 43.1 MPa, and the foundation stiffness of 0.8 m diameter circular bearing plate is 94 MPa/m, 60 MPa/m, 81 MPa/m, and the average value is 78.2 MPa/m. The mean values of 78.2 MPa/m can be used as a basis for the structural design of the corridor and the subsequent superstructure test calculations.

Through numerical simulation research found that the soil settlement deformation process and the pipe corridor relative displacement, the shear effect on both sides of the pipe corridor; differential settlement under the influence of the local surface of the pipe corridor may occur tensile damage, the maximum displacement concentrated in both sides of the pit reached 0.6 mm, in the acceptable range. Therefore, the lower base of the pipe corridor has good bearing capacity and can meet the construction requirements of the installation stage of the integrated pipe corridor sections. It is possible to avoid structural misalignment points and prevent The study will help similar projects in the future. This study will be useful for similar projects in the future. The study will be useful for similar projects in the future.

Data Availability

All data, models, and code generated or used during the study appear in the submitted article.

Conflicts of Interest

The authors declare that there are no conflicts of interest.

References

[1] Z. Tan, X. Chen, X. Wang, and M. Huang, "Construction management mode and key technology of urban underground integrated pipe corridor," *Tunnel construction*, vol. 36, no. 10, pp. 1177–1189, 2016.

[2] H. Wang, "Some problems in the construction of urban underground integrated pipe corridor projects in China," *Tunnel construction*, vol. 37, no. 05, pp. 523–528, 2017.

[3] Z. Jia, Z. Chen, and W. Li, "The present situation and development of urban underground comprehensive pipe gallery," *Jiangxi building materials*, vol. 2016, no. 22, pp. 6-7, 2016.

[4] B. Wang and S. Dai, "A brief discussion on the necessity of construction of underground integrated pipeline corridor in China's cities and its development prospects," *Anhui Architecture*, vol. 22, no. 6, p. 43+159, 2015.

[5] H. Zhou and Q. Jiang, "Preliminary interpretation of the guidance on promoting the construction of integrated urban underground pipe corridors," *Environment and Sustainable Development*, vol. 40, no. 05, pp. 58-59, 2015.

[6] F. Yang, "Preliminary discussion and analysis of construction methods for urban underground municipal integrated pipeline corridors," *Anhui architecture*, vol. 23, no. 3, pp. 88–91, 2016.

[7] X. You, "Status and development trend of urban integrated pipe corridor," *Urban housing*, vol. 24, no. 3, pp. 6–9, 2017.

[8] Y. Wang, "The development and outlook of urban underground multi-utility tunnel in China," *Engineering Technology Research*, vol. 2017, no. 8, pp. 244-245, 2017.

[9] Z. Tian, *Experimental Study on the Force Performance of Assembled Laminated concrete Underground Integrated Pipe Corridor*, Harbin Institute of Technology, Harbin, China, 2016.

[10] D. Kong, Y. Xiong, Z. Cheng, N. Wang, G. Wu, and Y. Liu, "Stability analysis of coal face based on coal face-support-roof system in steeply inclined coal seam," *Geomech. Eng.*vol. 25, pp. 233–243, 2021.

[11] L. Zhou, "Research on key technologies for the construction of safety monitoring system of urban underground integrated pipe corridor [J]," *Modern surveying and mapping*, vol. 39, no. 6, pp. 39–41, 2016.

[12] J. Yang and W. Wei, "Design and construction research of the urban underground pipe gallery structure," *Engineering Construction and Design*, vol. 2017, no. 6, pp. 19-20, 2017.

[13] X. Huang and X. Fan, "Analysis of the applicability of HS model in numerical simulation of foundation pit engineering," *Journal of Water Resources and Construction Engineering*, vol. 16, no. 2, pp. 115–120, 2018.

[14] X. Hu, S.-nan Fu, Lv Liang, C. Xiao-wen, and W. Xue, "Analysis of force performance of prefabricated assembled integrated pipe corridor under soft soil layer," *Construction Technology*, vol. 47, no. 12, pp. 118–121, 2018.

[15] Y. Wang, "A brief discussion on the design of urban underground integrated pipe corridor and the application of open excavation method construction technology," *Engineering quality*, vol. 34, no. S1, pp. 154–158, 2016.

[16] J. Ren, "A brief discussion on the necessity of urban underground integrated pipeline corridor," *Science and technology information*, vol. 12, no. 17, p. 63, 2014.

[17] H. Wu, G. Zhao, and S. Ma, "Failure behavior of horseshoe-shaped tunnel in hard rock under high stress: phenomenon and mechanisms," *Transactions of Nonferrous Metals Society of China*, vol. 32, no. 2, pp. 639–656, 2022.

[18] L. Sun, "An exploration of the structural design and construction of urban underground integrated pipeline corridors," *Science and technology wind*, no. 24, p. 152, 2012.

[19] S. Yao and Z. Wang, "Research on the construction technology of urban underground integrated pipe corridor," *Green environmental protection building, materials*, no. 01, p. 111, 2017.

[20] L. Dong and Z. Gao, "Exploration and practice of the sponge city construction in obsolete region," *Environmental Engineering*, vol. 37, no. 7, pp. 13–17, 2019.

[21] Y. Gong, Y. Chen, L. Yu et al., "Effectiveness analysis of systematic combined sewer overflow control schemes in the sponge city pilot area of beijing," *International Journal of Environmental Research and Public Health*, vol. 16, no. 9, p. 1503, 2019.

[22] L. Zhou, "Discussion on waterproofing design and construction method of urban underground comprehensive pipe gallery," *Jiangxi building materials*, vol. 2017, no. 22, p. 106–111, 2017.

[23] J. Cao, N. Zhang, S. Wang, D. Qian, and Z. Xie, "Physical model test study on support of super pre-stressed anchor in the mining engineering," *Engineering Failure Analysis*, vol. 118, Article ID 104833, 2020.